NeuroImage 211 (2020) 116629

Contents lists available at ScienceDirect

NeuroImage

journal homepage: www.elsevier.com/locate/neuroimage

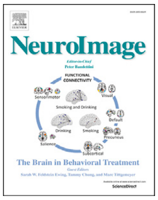

One bad apple spoils the whole bushel: The neural basis of outlier processing

Jonathan S. Cant [a,*], Yaoda Xu [b]

[a] Department of Psychology, University of Toronto Scarborough, Toronto, ON, M1C 1A4, Canada
[b] Department of Psychology, Yale University, New Haven, CT, 06477, USA

ARTICLE INFO

Keywords:
Object-ensemble perception
Outlier perception
Scene perception
fMRI
Ventral visual stream

ABSTRACT

How are outliers in an otherwise homogeneous object ensemble represented by our visual system? Are outliers ignored because they are the minority? Or do outliers alter our perception of an otherwise homogeneous ensemble? We have previously demonstrated ensemble representation in human anterior-medial ventral visual cortex (overlapping the scene-selective parahippocampal place area; PPA). In this study we investigated how outliers impact object-ensemble representation in this human brain region as well as visual representation throughout posterior brain regions. We presented a homogeneous ensemble followed by an ensemble containing either identical elements or a majority of identical elements with a few outliers. Human participants ignored the outliers and made a same/different judgment between the two ensembles. In PPA, fMRI adaptation was observed when the outliers in the second ensemble matched the items in the first, even though the majority of the elements in the second ensemble were distinct from those in the first; conversely, release from fMRI adaptation was observed when the outliers in the second ensemble were distinct from the items in the first, even though the majority of the elements in the second ensemble were identical to those in the first. A similarly robust outlier effect was also found in other brain regions, including a shape-processing region in lateral occipital cortex (LO) and task-processing fronto-parietal regions. These brain regions likely work in concert to flag the presence of outliers during visual perception and then weigh the outliers appropriately in subsequent behavioral decisions. To our knowledge, this is the first time the neural mechanisms involved in outlier processing have been systematically documented in the human brain. Such an outlier effect could well provide the neural basis mediating our perceptual experience in situations like “one bad apple spoils the whole bushel”.

1. Introduction

How are outliers represented in the brain? On the one hand, outliers can be salient and affect the quality of our experience, such as when one bad apple spoils the whole bushel. On the other hand, we may ignore outliers and discount their influence, such as ignoring the few leaves randomly mixed in with a box of fresh raspberries. Here we show that the presence of outliers significantly alters the neural representations of object ensembles in multiple human cortical regions despite a task that required participants to actively ignore outliers.

There has been increasing interest in the cognitive mechanisms mediating the processing of large collections, or ensembles, of multiple objects (Whitney and Leib, 2018). The visual system appears to capitalize on the redundancy of ensembles by forming a compressed statistical representation of the world when processing visual information (Balas et al., 2009; Oliva and Torralba, 2001; Rosenholtz, 2011; Rosenholtz et al., 2012). This representation can take the form of a summary statistic of the image, such as the mean size of circles (Ariely, 2001), the mean orientation of lines (Dakin and Watt, 1997), the mean identity or expression of a crowd of faces (de Fockert and Wolfenstein, 2009; Haberman and Whitney, 2007), and the mean lifelikeness of a group of objects (Yamanashi Leib et al., 2016).

Consistent with our ability to ignore outliers, Haberman and Whitney (2010) demonstrated that judgments of the mean emotional expression of a set of 12 faces containing 2 deviant expressions were made by discounting the outlier faces. Specifically, participants’ reports of mean expression were more sensitive to the local mean of the set (the mean expression of the 10 faces that were not outliers) compared with the global mean (the mean expression of all 12 faces). Since outliers increase the variability of a set and potentially make estimates of the mean less

---

* Corresponding author. 1265 Military Trail, Science Wing Room 411, Toronto, ON, M1C 1A4, Canada.
E-mail address: jonathan.cant@utoronto.ca (J.S. Cant).

https://doi.org/10.1016/j.neuroimage.2020.116629
Received 9 October 2019; Received in revised form 1 February 2020; Accepted 9 February 2020

reliable (Haberman and Whitney, 2010), discounting outliers may have adaptive value in visual perception. Despite our ability to ignore outliers, there are situations in which outliers can dominate visual experience, such as in visual feature search when an outlier item “pops out” from the set it is contained within (Treisman and Gelade, 1980). Recent studies have also demonstrated that, in addition to the mean, the range of a set is also implicitly extracted in ensemble perception (Khayat and Hochstein, 2018), and the outer boundaries of the range are used to detect outliers (Hochstein et al., 2018). Thus, outliers may not always be discounted in ensemble perception, since their presence may represent important information that may be relevant to the planning of future actions within our environment.

Less is known about the neural substrates mediating object-ensemble perception. In the first neuroimaging study to investigate this, we used functional magnetic resonance imaging adaptation (fMRI-A) and found that anterior-medial visual regions (in parahippocampal cortex) are sensitive to processing object ensembles (Cant and Xu, 2012). These regions have been associated with texture (Cant et al., 2009; Cant and Goodale, 2007, 2011; Peuskens et al., 2004) and scene processing (in the parahippocampal place area, or PPA; Epstein and Kanwisher, 1998). The existence of ensemble processing in this region is likely because ensemble, texture, and scene processing all rely on the extraction of statistical visual information (e.g., compressing visual redundancies into summary statistical representations). In subsequent studies we discovered that ensemble representation in PPA was sensitive to processing the ratio and identity of different objects comprising a heterogeneous ensemble (Cant and Xu, 2015), and the shape and texture of ensemble elements (Cant and Xu, 2017). Interestingly, PPA was not sensitive to processing ensemble features such as density, colour, and spatial frequency. This suggests that ensemble representation in anterior-medial ventral visual cortex is based on mid-to high-level, rather than low-level, visual information. Meanwhile, we did not observe robust and consistent ensemble sensitivity in other scene-selective cortical areas, namely, the retrosplenial complex (RSC) and occipital place area (OPA). We also found that the lateral occipital area (LO) processes shape from local ensemble elements, suggesting that in addition to its role in processing the shape of single objects (Grill-Spector et al., 1999; Kourtzi and Kanwisher, 2001; Malach et al., 1995), LO extracts shape out of more cluttered and ecologically valid images (Cant and Xu, 2012, 2015; 2017).

In the present study, we examined the impact of outliers on ensemble representation using an fMRI-adaptation paradigm, wherein participants were presented with a homogeneous ensemble containing 25 identical elements followed by another ensemble containing a majority of identical elements with 0 (i.e., also homogeneous, with no outliers), 2, or 4 outliers. Participants were asked to ignore the outliers and judge whether the two ensembles were mostly the same or different. For same judgments, the majority of the elements in the second ensemble were identical to those in the first, except for the outliers which were visually distinct. For different judgments, the majority of the elements in the second ensemble were distinct from those in the first, except for the outliers which were identical to those in the first ensemble. If outliers are effectively ignored due to the demands of the task and their minority status in the ensemble, then we should see insensitivity to processing outliers in a brain region (i.e., adaptation in all same-judgment trials, and a release from adaptation in all different-judgment trials). If, however, outliers dominate perception because their presence changes the nature of an otherwise homogeneous ensemble, then we should see sensitivity to the presence of outliers in a brain region (i.e., a release from adaptation in same-judgment trials, and adaptation in different-judgment trials, as outliers are introduced). We examined how the presence of outliers affects the representation of ensembles in anterior-medial ventral visual cortex (i.e., PPA). In addition to PPA, we examined cortical regions that play different roles in various aspects of visual processing (i.e., RSC, OPA, early visual cortex, or EVC, LO, and the fusiform face area, or FFA), as well as in posterior parietal cortex (PPC), and asked whether the effect of outliers are specific to PPA, or are more general and wide-spread.

2. Materials and methods

2.1. Participants

Fifteen paid participants took part in this study (10 female, 5 male; mean age = 27.07, range = 20–35 years), all of whom were recruited from the Harvard University community, and all were right-handed, reported normal color vision, normal or corrected-to-normal visual acuity, had no history of neurological disorder, and gave their informed consent to participate in the study in accordance with the Declaration of Helsinki. The experiments were approved by the Committee on the Use of Human Subjects at Harvard University.

Two additional participants took part in the study but were excluded from further analysis due to either significant head motion during the experiment (i.e., translations and rotations in excess of 3 mm and 3°, respectively) or very poor behavioral performance in the adaptation task (see *Behavioral data analysis* for more details), rendering their fMRI data unreliable and difficult to interpret. Importantly, a power analysis revealed that the total sample size required for our study (one-way repeated measures ANOVA with 6 levels of the factor ‘Condition’, see ‘Statistical analysis’ for more details), assuming a large effect size (0.4) based on Cohen’s f, an alpha level of 0.01, and a power value of 0.95, is 15 participants. Given that we consistently see large effect sizes in our previous fMRI studies of ensemble processing (effect sizes for our three previous fMRI studies are given in the Supplementary Results) and our sample size in this study is 15, we feel that we are sufficiently powered to detect significant effects.

2.2. Stimuli and experimental design

Adaptation experiment A fast event-related fMRI-adaptation paradigm, as was used in Cant and Xu (2012, 2015, 2017), was used in this experiment. Each trial contained a sequential presentation of 2 images and participants were asked to compare the two stimuli and make a same/different judgment relating the majority of similar items in the second ensemble to the items in the first (see below and Fig. 1A for more details).

The stimulus set for each participant was generated online, with the constraint that certain pairs of objects could not appear together if they were visually too similar in color and/or shape. Each stimulus set contained computer-generated object ensembles (25 objects in each ensemble) that were either entirely homogeneous (containing 25 repetitions of the same object) or mostly homogeneous (containing 23 or 21 repetitions of the same object, but with either two or four repetitions, respectively, of a second object which served as outliers; see Fig. 1B). The two types of objects in an ensemble were roughly the same size but were otherwise highly distinguishable from each other, and were drawn randomly from a pool of 40 different line-drawing objects (24 of which were man-made objects, and 16 of which were natural objects, i.e., fruits, vegetables, insects, and flowers). These 40 objects were a subset of the colored line-drawing objects developed by Rossion and Pourtois (2004). Since objects appeared in different orientations in the ensemble, only objects that could naturally appear in random orientations were included in our set of 40 objects. Altogether, our object pairs were chosen from 540 possible pairs of highly distinctive objects. All images subtended 12.5° × 12.5° of visual angle (this also applied to all the images used in the object/face/scene localizer).

There were a total of 6 stimulus conditions (Fig. 1A): (1) Same – 0 outliers (Same0): the same homogeneous ensemble image, with no outliers, was presented two times successively; (2) Same – 2 outliers (Same2): 23 of the elements in the second ensemble were identical to those in the first, except for 2 outliers which were visually distinct; (3) Same – 4 outliers (Same4): 21 of the elements in the second ensemble were identical to those in the first, except for 4 outliers which were visually distinct; (4) Different – 0 outliers (Different0): two distinct homogeneous ensemble images (each with no outliers) were presented successively; (5) Different – 2 outliers (Different2): 23 of the elements in the second ensemble were distinct from those in the first, except for 2 outliers which were identical to the objects in the first ensemble; and (6) Different – 4 outliers (Different4): 21 of the elements in the second ensemble were distinct from those in the first, except for 4 outliers which were identical to the objects in the first ensemble.

Each trial lasted 6 s, beginning with a 500 ms fixation, followed by two successively presented images (each presented for 500 ms, with a 300 ms blank fixation in between), and ending with a 4200 ms blank response screen. Participants were asked to ignore the outliers and judge whether the two ensembles were mostly the same or different by pressing the appropriate response button with their right index or middle finger, respectively (with conditions 1, 2, and 3 requiring a 'same' response, and conditions 4, 5, and 6 requiring a 'different' response). In addition to the stimulus trials, there was also 6-s blank fixation trials in which no images were presented. Trial order was pseudorandom and balanced for trial history (e.g. trials from all conditions including fixation were preceded and followed equally often by trials from all the conditions, including itself, for one trial back and forward; see Kourtzi and Kanwisher, 2001; Xu and Chun, 2006; Cant and Xu, 2012, 2015, 2017). To balance the trial order for the first and last trials in each sequence, two 6 s filler trials were also added, with one at the beginning and one at the end of the sequence. These filler trials were removed during data analysis. There was also a 3 s fixation period at the beginning of the run to orient participants' attention to the display before the onset of the visual stimuli. Each run ended with another 3 s fixation period. To further balance trial history, trial order was rotated among the conditions in different runs and among different participants. Each adaptation run lasted 5 min and 12 s and contained 7 trials for each stimulus condition. All participants took part in four adaptation runs.

Object/Face/Scene localizer The stimuli used to localize object-, face-, and scene-sensitive areas of cortex consisted of photographs of various indoor and outdoor scenes (e.g. furnished rooms, buildings, city landscapes, and natural landscapes), both male and female faces, common objects (e.g. cars, chairs, food, and tools), and phase-scrambled versions of the common objects.

A single run consisted of presenting four blocks each of scenes, faces, intact objects and phase-scrambled objects. Each stimulus block was 16-s long and contained 20 different images, each lasting 750 ms and followed by a 50 ms blank period. No images were repeated within or across blocks in a given run. To ensure attention to the displays, participants fixated at the center and detected a slight spatial jitter, occurring randomly in 1 out of every 10 images. In addition to the stimulus blocks, there were also 8-s fixation blocks presented at the beginning, middle, and end of each run. Following Kanwisher et al. (1997) and Epstein and Kanwisher (1998), we used two unique and balanced run orders. Each run lasted 4 min and 40 s. All participants took part in three runs of this localizer.

2.3. *Apparatus*

Stimulus presentation and the collection of behavioral responses (via a response pad placed in the participant's right hand) were controlled by an Apple MacBook Pro (Apple Corporation, California, USA) running MATLAB with Psychtoolbox extensions (Brainard, 1997; Pelli, 1997). Each image was rear projected via an LCD projector (Sharp Notevision XG-C465X, resolution of 1024 × 768, Sharp Corporation, Pennsylvania, USA) onto a screen mounted behind the participant as he or she lay in the scanner bore. The participant viewed the images through an angled mirror mounted to the head coil directly above the eyes.

2.4. *Imaging parameters*

This study was conducted on a 3.0 Tesla Siemens MAGNETOM Tim Trio (Erlangen, Germany) whole-body imaging MRI system at the Center for Brain Science, Harvard University (Cambridge, Massachusetts, USA). A Siemens radio-frequency (RF) 32-channel head coil was used to collect BOLD weighted images (Ogawa et al., 1992). For high-resolution anatomical images, T1-weighted 3-D magnetization prepared rapid acquisition gradient echo (MPRAGE) sagittal slices covering the whole brain were collected (inversion time 1100 ms, echo time, or TE, 1.54 ms, repetition time, or TR, 2200 ms, flip angle 7°, 256 × 256 matrix size, 144 slices, 1.0 mm × 1.0 mm x 1.0 mm voxel size). For the functional runs, a

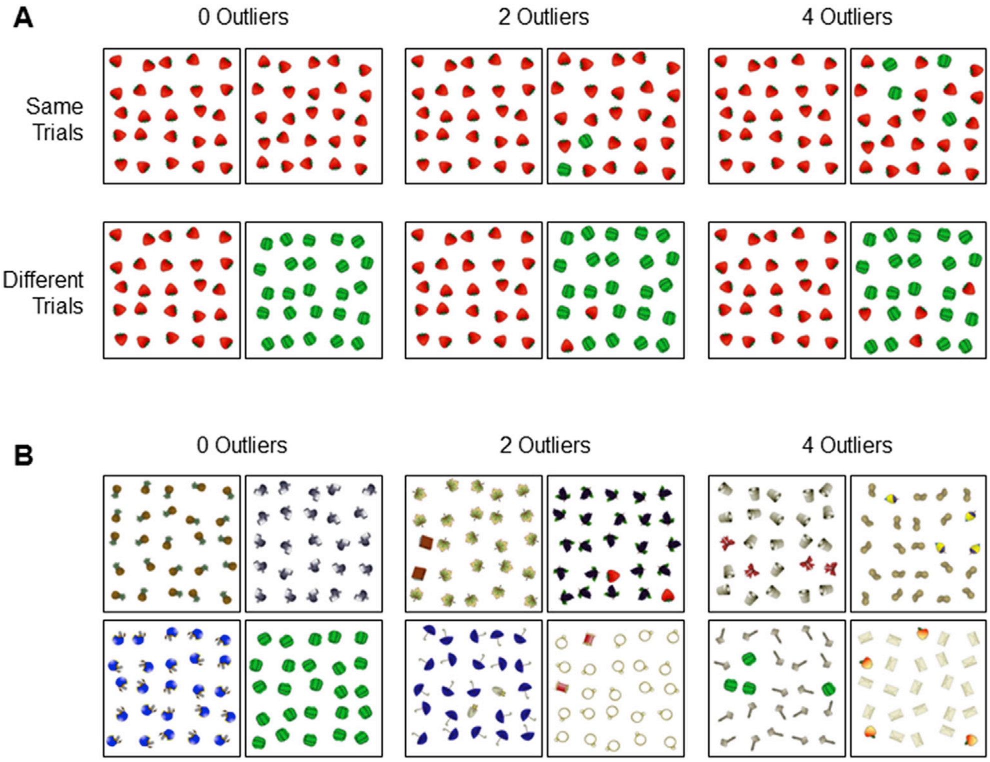

Fig. 1. Example stimuli and conditions used in the fMRI adaptation experiment. **A.** Example stimuli for all 6 adaptation conditions used in the experiment. Each ensemble stimulus contained full-color cartoon objects (25 objects in each ensemble) that were either entirely homogeneous (containing 25 repetitions of the same object) or mostly homogeneous (containing 23 or 21 repetitions of the same object, but with either two or four repetitions, respectively, of a second object which served as outliers). Each trial contained a sequential presentation of 2 images and participants were asked to ignore the outliers and judge whether the two ensembles were mostly the same (the three conditions in the same trials) or different (the three conditions in the different trials). **B.** Additional examples of the ensembles used in the 0 outlier, 2 outliers, and 4 outliers conditions.

T2*-weighted echo-planar gradient echo pulse sequence (72 × 72 matrix size, field of view 21.6 cm) with TR of 1.5 s was used in the adaptation experiment (TE 29 ms, flip angle 90°, 208 vol). Another pulse sequence with TR of 2.0 s was used for the localizer runs (TE 30 ms, flip angle 85°, 140 vol). Twenty-four 5-mm-thick (3 mm × 3 mm in-plane, 0 mm skip) slices parallel to the anterior and posterior commissure line were collected in all the functional runs.

2.5. Statistical analysis

fMRI data analysis fMRI data were analyzed with Brain Voyager QX (Brain Innovation, Maastricht, The Netherlands). Data pre-processing included slice acquisition time correction, 3D motion correction, linear trend removal, and Talairach space transformation (Talairach and Tournoux, 1988).

Data from the object/face/scene localizer was analyzed using a general linear model (GLM), accounting for hemodynamic lag (Friston et al., 1995). Following Epstein and Kanwisher (1998), the PPA ROI was defined as regions in the collateral sulcus and parahippocampal gyrus whose activations were higher for scenes than for faces and objects (false discovery rate $q < 0.05$; this threshold applies to all functional regions localized in individual participants) (see Fig. 2A). Following Epstein and Higgins (2007) and Dilks et al. (2013), the RSC and OPA ROIs were defined as regions in restrosplenial cortex-posterior cingulate-medial parietal cortex, and transverse occipital cortex, respectively, whose activations were higher for scenes than for faces and objects. Following known anatomical criteria and the procedure established in a number of previous studies (e.g., Grill-Spector et al., 1999; James et al., 2003; MacEvoy and Epstein, 2011; Cant and Xu, 2015), retinotopic EVC was defined as a region around the Calcarine sulcus that showed higher activation for scrambled compared with intact objects. Following Grill-Spector et al. (2000), LO was defined as a region in lateral occipital cortex near the posterior inferotemporal sulcus whose activations were higher for intact objects than for phase-scrambled objects. Following Kanwisher et al. (1997), the FFA was defined as a region in extrastriate cortex along the fusiform gyrus that showed higher activation for faces than scenes and objects. Finally, two regions were localized in PPC using separate sets of imaging data. The first, PPC1, was localized individually in each participant using the object/face/scene localizer and was defined as a region that showed greater activation for intact compared with scrambled objects. This region was generally located along the superior portion of the intraparietal sulcus in each participant. The second region, PPC2, was localized using the group adaptation data from all 15 participants and was defined as a region that showed greater activation for all 6 adaptation conditions compared with baseline fixation (at a false discovery threshold of $q < 0.001$ owing to the large amount of activation observed with this contrast; PPC1 was defined using the same threshold to facilitate comparisons across both parietal regions). We used group data to define PPC2 because initially we were not able to localize a PPC region consistently in each participant using their respective adaptation data. This group region was projected onto each participant's brain separately and was generally located more laterally and slightly anterior than each participant's individual PPC1. Because PPC2 differed in its spatial location from PPC1 (with no overlapping voxels between the ROIs), for completeness, we included both PPC ROIs in our analysis. All regions were successfully identified in both hemispheres separately for each individual that took part in the study, with the exception of OPA which was identified bilaterally in 14 of the 15 participants, and PPC2 which was defined bilaterally using a single contrast based on the group data.

Following the standard ROI-based analysis approach (see Saxe et al., 2006), we overlaid the ROIs from each participant onto their data from the main adaptation experiment and extracted time courses from that participant. The averaged activation levels for all conditions were then extracted and converted to percentage BOLD signal change from baseline, by subtracting the corresponding activation from the fixation trials and then dividing by this value (see Kourtzi and Kanwisher, 2001; Todd and Marois, 2004; Xu and Chun, 2006; Xu, 2010; Dilks et al., 2011; Todd et al., 2011; Cant and Xu, 2012, 2015; 2017). Peak responses for each condition were obtained by collapsing the time courses for all of the conditions and then identifying the time point of greatest signal amplitude in the average response, thereby ensuring that the time point selected was not biased to the level of activation for any one condition in particular (e.g., Xu and Chun, 2006; Xu, 2010; Cant and Xu, 2012, 2015; 2017; see Supplementary Results for the raw time course data). This was done separately for each participant in each ROI, and these resulting peak responses were then averaged across all participants.

We examined sensitivity to processing outliers using the following five steps. First, we conducted a 2 × 6 repeated measures ANOVA to examine whether activation for the adaptation conditions differed across hemispheres in each ROI separately (SPSS, Chicago, Illinois, USA), with main effects of Hemisphere (left vs. right) and Condition (6 adaptation conditions). If there was no evidence for a difference in activation for the adaptation conditions across hemispheres (i.e., a non-significant Hemisphere-by-Condition interaction), then data from the left and right hemispheres was collapsed for all subsequent analyses. Second, we examined the average levels of activation for each adaptation condition using a single factor (Condition: 6 adaptation conditions) repeated measures ANOVA, performed separately on each ROI. Third, we conducted a posthoc pairwise comparison looking specifically for the expected general adaptation effect, that is, significantly greater activation in the Different0 condition compared with the Same0 condition. Critically, failing to find the expected adaptation effect makes it significantly less likely that a given region will demonstrate sensitivity to processing outliers. Fourth, we conducted posthoc pairwise comparisons to examine if there was a significant release from adaptation in same-judgment trials as outliers were introduced (i.e., Same0 vs. Same2, Same0 vs. Same4, and Same2 vs. Same4) and adaptation in different-judgment trials as outliers were introduced (i.e., Different0 vs. Different 2, Different0 vs. Different4, and Different2 vs. Different4). Posthoc pairwise comparisons (all two-tailed) were conducted using the Bonferroni procedure to control for inflations to Type 1 error as a result of multiple statistical comparisons. Fifth, we also conducted 2 × 6 repeated measures ANOVAs to examine if the adaptation results differed across ROIs, with main effects of Region (e.g., PPA vs. LO) and Condition. All analyses used alpha = 0.05.

Finally, we conducted whole-brain random-effects analyses on the entire group of participants (at $P < 0.01$, uncorrected, since very little activation was observed at $P < 0.001$, uncorrected) and also on subsets of participants (i.e., one group of participants that showed a strong behavioral response-latency effect, and another group that showed a weak response-latency effect, $N = 8$ and $N = 7$, respectively; both at $P < 0.05$, uncorrected owing to the small sample sizes), to examine sensitivity to processing ensemble outliers across the entire brain.

Behavioral data analysis Behavioral performance measures of response latency and accuracy for the adaptation runs were recorded by MATLAB (running the Psychtoolbox) and were analyzed with SPSS (Chicago, Illinois, USA; see below).

Before data were analyzed, two analyses were performed to remove outliers. First, participants were excluded from further analysis if their average accuracy across conditions was less than 2.5 standard deviations below the grand mean for accuracy (76.46%), which was a good indication that the participant was not properly engaged in the task, making their data unreliable and difficult to interpret. This resulted in the removal of one participant. Second, for the remaining participants, following standard practice, response latencies that were 2.5 standard deviations above or below the mean reaction time for each stimulus condition were excluded from each participant separately.

Response latencies (for correct trials only) and the number of errors committed in the adaptation runs were analyzed using a single factor (Condition: 6 adaptation conditions) repeated measures ANOVA (both with alpha = 0.05). Similar to the fMRI analysis, all posthoc pairwise comparisons were two-tailed and were conducted using the Bonferroni

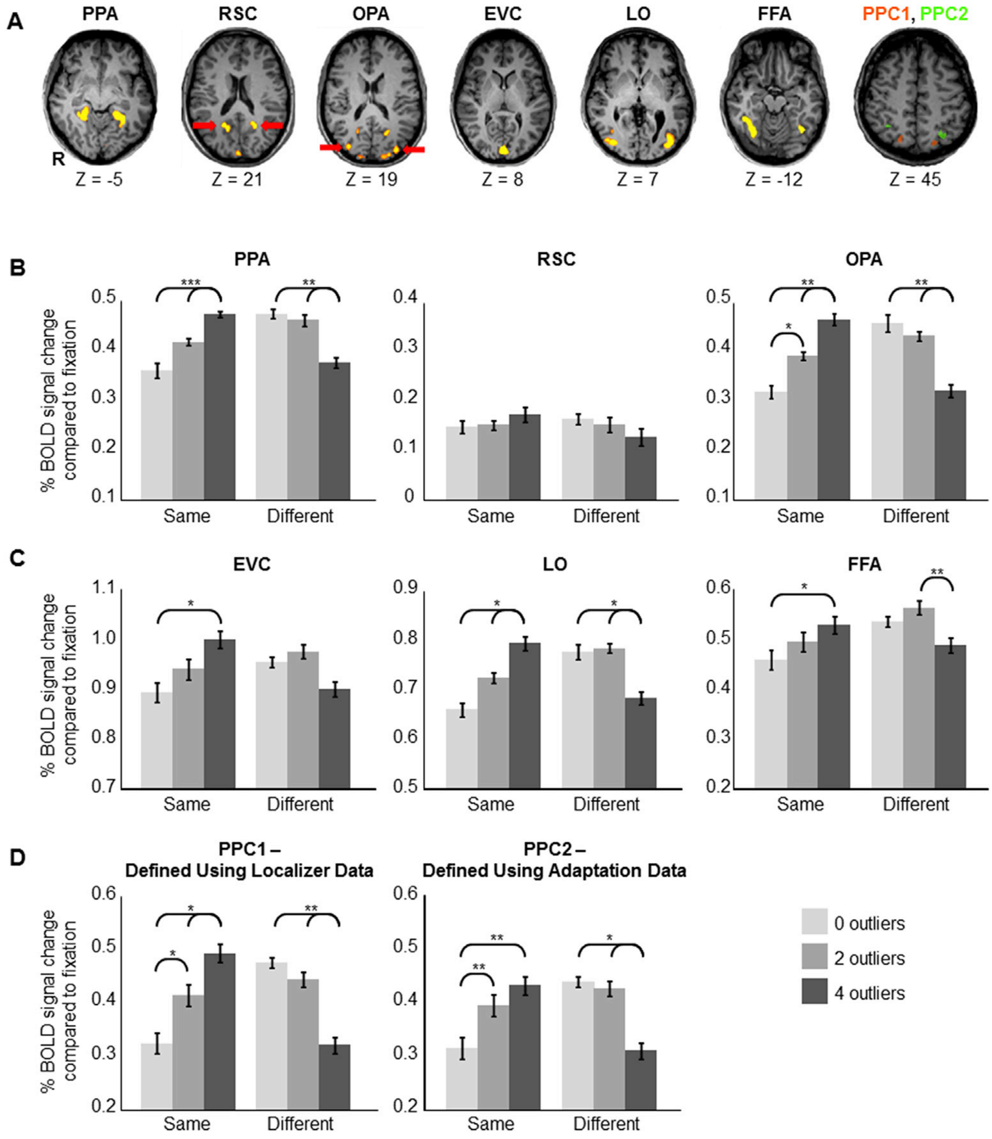

Fig. 2. Cortical Regions and results (N = 15) of the ROI analysis for all six fMRI adaptation outlier conditions in all eight ROIs. **A.** Illustrative examples of the regions targeted in the ROI analysis. The scene-selective PPA (Talairach x, y, z, coordinates for right/left: +22/-23, −40/-40, −5/-5) was defined by contrasting the activation for scenes against the activation for both faces and objects. The scene-selective RSC (+17/-20, −56/-53, +22/+18) and OPA (+35/-33, −78/-83, +10/+17) were defined using the same contrast as PPA. Early visual cortex (0, −86, 8) was defined by contrasting the activation for phase-scrambled objects against the activation for intact objects. The object-selective LO (+33/-35, −75/-75, +2/+2) was defined by contrasting the activation for objects against the activation for phase-scrambled objects. The face-selective FFA (+34/-35, −52/-52, −12/-8) was defined by contrasting the activation for faces against the activation for both scenes and objects. PPC1 was defined in each participant separately using the object/face/scene localizer (shown in orange, from a representative participant; Talairach x, y, z, coordinates for right/left: +21/-21, −65/-70, 43/45) using a contrast of higher activation to intact compared with scrambled objects. PPC2 was defined based on the adaptation data from all 15 participants (shown in green, and projected onto the same representative participant's brain; +30/-30, −50/-60, 43/44) using a contrast of higher activation for all 6 adaptation conditions compared with baseline fixation. Both regions were localized at an FDR-corrected threshold of $q < 0.001$. **B & C.** Results in PPA, RSC, OPA, EVC, LO, and FFA. In PPA, there was a general expected adaptation effect (i.e., Different0 > Same0), a release from adaptation in same-judgment trials when 2 and 4 outliers were present, and adaptation in different-judgment trials when 4 outliers were present. Interestingly, the release from adaptation in same-judgment trials with 4 outliers was very similar to that seen in different-judgment trials where two completely different ensembles were presented, and the adaptation in different trials with 4 outliers was comparable to that seen in same-judgment trials where the same ensemble with no outliers is repeated. Similar results were observed in OPA and LO, in that both regions showed a general adaptation effect, release from adaptation in same-judgment trials when 4 outliers were present, and adaptation in different-judgment trials when 4 outliers were present. Thus, PPA, OPA, and LO all show a strong outlier effect. In contrast, despite the overall response patterns resembling those of PPA, OPA and LO, little-to-no statistically significant sensitivity to the outlier effect was observed in RSC, EVC, and FFA (i.e., no general adaptation effect and far fewer critical pairwise comparisons showing significance). **D.** Results in PPC1 and PPC2 were very similar to each other, and also to the results observed in PPA, OPA, and LO: a general adaptation effect, a release from adaptation in same-judgment trials when 2

and 4 outliers were present, and adaptation in different-judgment trials when 4 outliers were present. Error bars represent within-subject standard errors (i.e. with the between-subject variation removed; see Loftus and Mason, 1994). R = right hemisphere; PPA = parahippocampal place area; RSC = retrosplenial complex; OPA = occipital place area; EVC = early visual cortex; LO = lateral occipital area; FFA = fusiform face area; PPC1 = posterior parietal cortex region 1; PPC2 = posterior parietal cortex region 2; BOLD = blood oxygen level dependent; * $P < 0.05$; ** $P < 0.01$; *** $P < 0.001$.

procedure.

2.6. Data and code availability

Data and code are freely available by contacting either Jonathan S. Cant (jonathan.cant@utoronto.ca) or Yaoda Xu (yaoda.xu@yale.edu).

3. Results

(1) The processing of outliers in PPA

We first examined outlier processing in PPA as this brain region has previously been shown to be involved in object ensemble processing (Cant and Xu, 2012, 2015, 2017). Because results in PPA did not differ across hemispheres (i.e., a non-significant Hemisphere-by-Condition interaction: $F_{5,70} = 1.24$, $P = 0.30$, $\eta_p^2 = 0.08$), data from the two hemispheres were averaged together for subsequent analyses. To evaluate the contribution of outliers, we conducted a single factor (Condition: 6 adaptation conditions) repeated measures ANOVA. This analysis revealed a significant main effect of Condition ($F_{5,70} = 20.20$, $P = 2.0 \times 10^{-12}$, $\eta_p^2 = 0.59$). In the first step of conducting posthoc pairwise comparisons (all two-tailed and Bonferroni corrected), we found a significant expected general adaptation effect (i.e., Different0 > Same0; $t_{14} = 5.43$, $P = 0.001$, Cohen's D = 1.40; see Fig. 2B), validating the further exploration of outlier sensitivity in PPA. Subsequent pairwise comparisons revealed that the Same4 condition had a significant release from adaptation compared with both the Same0 ($t_{14} = 7.53$, $P = 4.3 \times 10^{-5}$, Cohen's D = 1.94) and the Same2 ($t_{14} = 6.36$, $P = 2.8 \times 10^{-4}$, Cohen's D = 1.63) conditions, and the Same2 condition demonstrated a marginally significant release from adaptation compared with the Same0 condition ($t_{14} = 3.24$, $P = 0.09$, Cohen's D = 0.84; see Fig. 2B). For different responses, the Different4 condition demonstrated significant adaptation (i.e., less activation) compared with both the Different0 ($t_{14} = 7.21$, $P = 6.8 \times 10^{-5}$, Cohen's D = 1.86) and Different2 ($t_{14} = 5.03$, $P = 0.003$, Cohen's D = 1.29) conditions, which did not differ from each other ($t_{14} = 0.76$, $P > 0.99$, Cohen's D = 0.19). Thus 4 and, to a lesser extent, 2 outliers are able to produce a release from adaptation in same judgments, and the presence of 4 outliers led to significant adaptation in different judgments. Interestingly, the release from adaptation in same-judgment trials with 4 outliers was quite similar to that seen in different-judgment trials where two completely different ensembles were presented (Same4 vs. Different0: $t_{14} = 0.05$, $P > 0.99$, Cohen's D = 0.01), despite the presence of multiple repeated items in the former condition (see Fig. 2B). Moreover, the adaptation in different trials with 4 outliers was comparable to that seen in same-judgment trials where the same ensemble with no outliers is repeated (Different4 vs. Same0: $t_{14} = 0.78$, $P > 0.99$, Cohen's D = 0.20), which is surprising given the limited number of repeated items in the former condition. Taken together, these results reveal that outliers significantly impact the neural representation of otherwise homogeneous ensembles in human anterior-medial ventral visual cortex, such that the presence of a few outliers can either cause a complete release from adaptation in an otherwise identical object ensemble or complete adaptation in an otherwise dissimilar object ensemble.

(2) The processing of outliers in the broader scene-processing network

To examine if the findings in PPA generalize to other scene processing cortical regions, we examined outlier processing in RSC and OPA. In RSC, the Hemisphere-by-Condition interaction was significant ($F_{5,70} = 2.64$, $P = 0.03$, $\eta_p^2 = 0.16$). While this does represent evidence that the adaptation results in RSC differ across hemispheres, to better compare with the results in PPA, which did not demonstrate hemispheric differences (as well as all other ROIs, see below), we combined data from the right and left RSC (but see Supplementary Results and Table 2 for the results of each hemisphere separately, which were similar to the results for the combined RSC reported below in terms of the main effects, pairwise posthoc comparisons, and the interactions with the other brain regions). The main effect of condition was not significant ($F_{5,70} = 1.06$, $P = 0.39$, $\eta_p^2 = 0.07$), and no pairwise comparison reached significance (all *t*s < 1.77, all *P*s > 0.99, all Cohen's Ds < 0.46; see Fig. 2B). These results demonstrate that the presence of outliers does not impact processing in RSC, which differs from the results observed in PPA. To provide empirical support for this observation, we compared the processing in RSC to the adaptation results in PPA using a 2 (Region: RSC vs. PPA) x 6 (Condition) repeated measures ANOVA and found a significant Region-by-Condition interaction ($F_{5,70} = 8.66$, $P = 2.0 \times 10^{-6}$, $\eta_p^2 = 0.38$), demonstrating that the findings in RSC significantly differ from those in PPA. This is further evidence that outliers do not alter the representation in this cortical region, and more generally, that RSC is not sensitive to processing object ensembles, which replicates our previous findings (Cant and Xu, 2012, 2015, 2017).

We found no evidence of hemispheric differences in the processing of ensemble outliers in OPA ($F_{5,65} = 0.81$, $P = 0.55$, $\eta_p^2 = 0.064$), and thus collapsed the data across hemispheres for subsequent analyses. In OPA, the main effect of Condition was significant ($F_{5,65} = 22.75$, $P = 4.1 \times 10^{-13}$, $\eta_p^2 = 0.64$), as was the general adaptation effect (i.e., Different0 > Same0; $t_{13} = 5.05$, $P = 0.003$, Cohen's D = 1.35; see Fig. 2B). Further pairwise posthoc comparisons for same judgments revealed that the Same2 and Same4 conditions both showed a significant release from adaptation compared with activation in the Same0 condition (Same2 vs. Same0: $t_{13} = 4.11$, $P = 0.018$, Cohen's D = 1.10; Same4 vs. Same0: $t_{13} = 7.69$, $P = 5.1 \times 10^{-5}$, Cohen's D = 2.06), and an additional release from adaptation was observed in the Same4 condition compared with the Same2 condition ($t_{13} = 4.85$, $P = 0.005$, Cohen's D = 1.30). For different judgments, the amount of activation observed in the Different0 and Different2 conditions did not differ ($t_{13} = 1.19$, $P > 0.99$, Cohen's D = 0.32), but both demonstrated a significant release from adaptation compared with the Different4 condition (Different0 vs. Different4: $t_{13} = 5.54$, $P = 0.001$, Cohen's D = 1.48; Different2 vs. Different4: $t_{13} = 6.71$, $P = 2.2 \times 10^{-4}$, Cohen's D = 1.79). The results in OPA are quite similar to those observed in PPA, and direct comparisons of OPA with PPA provided support for this (non-significant Region-by-Condition interaction: $F_{5,65} = 2.03$, $P = 0.09$, $\eta_p^2 = 0.14$). Finally, we compared the results in OPA and RSC and found significantly different adaptation results across these two scene-selective regions ($F_{5,65} = 11.08$, $P = 9.7 \times 10^{-8}$, $\eta_p^2 = 0.46$). Taken together, these results reveal that the presence of outliers in object ensembles has a similar effect on processing in two different scene-selective regions (i.e., PPA, OPA), but no effect in a third scene-processing region (i.e., RSC). This supports a functional dissociation in the processing of object ensembles within the human scene-selective network, consistent with our previous findings (Cant and Xu, 2012, 2015, 2017).

(3) The processing of outliers in other occipital regions

To examine if the findings in PPA and OPA generalize to other visual regions in occipital cortex, we examined outlier processing in EVC, LO and FFA. In EVC, since no effect of Hemisphere was found ($F_{5,70} = 0.85$, $P = 0.52$, $\eta_p^2 = 0.06$), data from left and right EVC were collapsed together. Similar to the findings in PPA and OPA, the main effect of Condition was significant ($F_{5,70} = 5.33$, $P = 3.3 \times 10^{-4}$, $\eta_p^2 = 0.28$). However, further pairwise posthoc comparisons revealed that the expected general adaptation effect was not significant (Different0 vs. Same0: $t_{14} = 2.41$, $P = 0.45$, Cohen's D = 0.62), and only one pairwise comparison was significant across both same- and different-judgment trials (a significant release from adaptation in the Same4 condition compared with the Same0 condition: $t_{14} = 3.91$, $P = 0.024$, Cohen's D = 1.01; all other ts < 3.32, all other Ps > 0.076, all other Cohen's Ds < 0.86; see Fig. 2C). While the interaction between brain region and adaptation condition was significant between EVC and OPA ($F_{5,65} = 3.31$, $P = 0.01$, $\eta_p^2 = 0.20$), this interaction was not significant between EVC and PPA ($F_{5,70} = 1.63$, $P = 0.16$, $\eta_p^2 = 0.10$).

We note that there exists a general response pattern that was shared among PPA, OPA and EVC, with Same0 lower than Same4, and Different0/Different2 greater than Different4. The presence of this general response pattern likely resulted in the region-by-condition interaction between PPA and EVC not being significant. Meanwhile, it is important to note that the basic adaptation effect was present in PPA and OPA but not in EVC, and that, of the 6 possible pairwise comparisons showing the outlier effect, the number of significant comparisons present were PPA – 4, OPA – 5, and EVC – 1. The presence of an additional significant pairwise comparison in OPA, but not in PPA, could have further differentiated the response patterns between OPA and EVC, making the region-by-condition interaction significant between those two brain regions. Taking both the interactions and pairwise comparisons into account, the overall results indicate that EVC was not particularly sensitive to processing ensembles and did not exhibit a robust outlier effect, even though its overall response profile may be similar to that of PPA.

In LO, the Hemisphere-by-Condition interaction was not significant ($F_{5,70} = 1.78$, $P = 0.13$, $\eta_p^2 = 0.11$) and thus data from the two hemispheres were combined. The main effect of Condition was significant ($F_{5,70} = 16.09$, $P = 1.57 \times 10^{-10}$, $\eta_p^2 = 0.54$), and similar to the results observed in PPA and OPA, the general adaptation effect was significant as well ($t_{14} = 4.77$, $P = 0.004$, Cohen's D = 1.23; see Fig. 2C). Further posthoc pairwise comparisons for same judgments revealed significant releases from adaptation for the Same4 compared with the Same0 ($t_{14} = 6.86$, $P = 1.2 \times 10^{-4}$, Cohen's D = 1.77) and Same2 ($t_{14} = 4.11$, $P = 0.016$, Cohen's D = 1.06) conditions. The difference in activation between the Same0 and Same2 conditions was not significant ($t_{14} = 3.03$, $P = 0.14$, Cohen's D = 0.78). For different judgments, the amount of activation observed in the Different0 and Different2 conditions did not differ ($t_{14} = 0.48$, $P > 0.99$, Cohen's D = 0.12), but both demonstrated a significant release from adaptation compared with the Different4 condition (Different0 vs. Different4: $t_{14} = 3.96$, $P = 0.021$, Cohen's D = 1.02; Differert2 vs. Different4: $t_{14} = 6.39$, $P = 2.5 \times 10^{-4}$, Cohen's D = 1.65). These results are similar to those observed in PPA and OPA, as the Region-by-Condition interaction was non-significant in both cases (both Fs < 1.89, both Ps > 0.10, both η_p^2s < 0.13).

To investigate if the outlier sensitivity observed in scene- and object-selective cortex is also found in high-level regions of the ventral stream that can be functionally dissociated from the processing in PPA, OPA, and LO, we examined sensitivity to processing ensemble outliers in FFA. Data from the right and left hemispheres was again collapsed since the Hemisphere-by-Condition interaction was non-significant ($F_{5,70} = 0.55$, $P = 0.74$, $\eta_p^2 = 0.04$). In FFA, the main effect of Condition was significant ($F_{5,70} = 6.59$, $P = 4.50 \times 10^{-5}$, $\eta_p^2 = 0.32$). Pairwise posthoc comparisons revealed that the general adaptation effect was only marginally significant ($t_{14} = 3.47$, $P = 0.056$, Cohen's D = 0.90), and only two pairwise comparisons across same and different judgments were significant (Same0 vs. Same4: $t_{14} = 3.70$, $P = 0.036$, Cohen's D = 0.96; Different2 vs. Different4: $t_{14} = 5.33$, $P = 0.002$, Cohen's D = 1.38; see Fig. 2C). The pattern of adaptation results in FFA was significantly different from that observed in PPA, OPA, LO, and RSC (all Fs > 3.33, all Ps < 0.01, all η_p^2s > 0.19).

Taken together, strong sensitivity to processing ensemble outliers is present in brain regions involved in ensemble and shape processing, including PPA, OPA and LO (see Discussion regarding the role of OPA in ensemble and shape processing). Meanwhile, very weak evidence of outlier sensitivity was observed in EVC and FFA, and no evidence was observed in RSC, demonstrating that the robust outlier effect in PPA, OPA, and LO is not a general effect present in all visually responsive brain regions.

(4) The processing of outliers across the entire brain

To examine if the sensitivity to processing ensemble outliers is unique to regions within occipito-temporal cortex, or is instead a more general cognitive phenomena that can be found in multiple cortices, we conducted a whole-brain random-effects analysis using the data from all 15 participants (all regions reported are significant at $P < 0.01$, uncorrected; see Table 1). Specifically, we searched for regions that showed the two strongest adaptation effects we observed in our ROI analysis. That is, we conducted a conjunction analysis searching for regions that showed: 1) increased activation in the Same4 condition compared with the Same0 condition; and 2) increased activation in the Different0 condition compared with the Different4 condition.

We observe a large amount of activation in occipito-temporal (concentrated along the collateral sulcus/parahippocampal cortex, fusiform gyrus, and in the location of OPA) and posterior parietal (concentrated along the intraparietal sulcus, or IPS, and in the superior parietal lobule, or SPL) cortices. We also observe a smaller amount of activation in frontal cortex, along the superior frontal sulcus (SFS) (see Fig. 3A). No regions are active for the reverse contrasts (i.e., greater activation for the conditions that showed adaptation in our main ROIs).

In summary, the results of the whole-brain random-effects analysis demonstrate that the adaptation results we report in the ROI analysis are not idiosyncratic to occipito-temporal cortex but also include extensive activation in posterior parietal, and to a lesser extent, frontal, cortices. Given the ability of frontal and posterior parietal cortex to encode visual information in visual working memory and their involvement in task-related processing (Christophel et al., 2017; Xu, 2017, 2018a), it appears that these regions also show sensitivity to the outlier effect (see below for a more detailed analysis of the parietal activations).

(5) The processing of outliers in posterior parietal cortex

Recent studies have shown that the human PPC is involved in adaptive aspects of visual information processing, such as directly representing task-relevant information (Vaziri-Pashkam and Xu, 2017; see also Xu, 2018a and 2018b), and showing sensitivity to processing ensemble features from crowds of faces (Im et al., 2017). To investigate if PPC

Table 1
Results of the whole-brain random-effects analyses.

Contrast: Conjunction of Same4 > Same0 & Different0 > Different4

Cortical Region	Sample Size	Talairach Coordinates (x,y,z)	Threshold Value	*T*-value
Right FG/CoS/PC	15 (Whole Group)	26, −60, −10	$P < 0.01$	2.98
Left FG/CoS/PC	15 (Whole Group)	30, −54, −14	$P < 0.01$	2.98
Right OPA	15 (Whole Group)	30, −79, 13	$P < 0.01$	2.98
Left OPA	15 (Whole Group)	−30, −84, 12	$P < 0.01$	2.98
Right IPS/SPL	15 (Whole Group)	24, −61, 40	$P < 0.01$	2.98
Left IPS/SPL	15 (Whole Group)	−27, −64, 39	$P < 0.01$	2.98
Right SFS	15 (Whole Group)	24, −9, 49	$P < 0.01$	2.98
Left SFS	15 (Whole Group)	−24, −4, 45	$P < 0.01$	2.98
Right FG/CoS	7 (Weak RT Group)	21, −57, −12	$P < 0.05$	2.45
Left FG/CoS	7 (Weak RT Group)	−25, −42, −12	$P < 0.05$	2.45
Right OPA	7 (Weak RT Group)	33, −82, 8	$P < 0.05$	2.45
Left OPA	7 (Weak RT Group)	−33, −83, 8	$P < 0.05$	2.45
Right IPS	7 (Weak RT Group)	26, −72, 32	$P < 0.05$	2.45
Left IPS	7 (Weak RT Group)	−28, −72, 32	$P < 0.05$	2.45
Right SPL	7 (Weak RT Group)	28, −54, 47	$P < 0.05$	2.45
Left SPL	7 (Weak RT Group)	−30, −55, 47	$P < 0.05$	2.45
Right FG/CoS	8 (Strong RT Group)	21, −57, −12	$P < 0.05$	2.45
Left FG/CoS	8 (Strong RT Group)	−32, −59, −12	$P < 0.05$	2.45
Right OPA	8 (Strong RT Group)	29, −84, 8	$P < 0.05$	2.45
Left OPA	8 (Strong RT Group)	−30, −86, 8	$P < 0.05$	2.45
Right IPS	8 (Strong RT Group)	23, −68, 32	$P < 0.05$	2.45
Left IPS	8 (Strong RT Group)	−26, −70, 32	$P < 0.05$	2.45
Right SPL	8 (Strong RT Group)	24, −55, 47	$P < 0.05$	2.45
Left SPL	8 (Strong RT Group)	−31, −54, 47	$P < 0.05$	2.45

FG = fusiform gyrus; Cos = collateral sulcus; PC = parahippocampal cortex; OPA = occipital place area; IPS = intraparietal sulcus; SPL = superior parietal lobule; SFS = superior frontal sulcus.

represents task-relevant features from ensembles of objects, we localized two separate regions of PPC (see Fig. 2A) and examined the sensitivity to processing ensemble outliers in each.

The first region, PPC1, was localized individually in each participant using the object/face/scene localizer and was defined as a region that showed greater activation to intact compared with scrambled objects. Data from the right and left hemispheres was collapsed since there was no evidence of differences in adaptation across hemispheres ($F_{5,70} = 1.78$, $P = 0.13$, $\eta_p^2 = 0.11$). The main effect of Condition was significant ($F_{5,70} = 18.64$, $P = 10.00 \times 10^{-12}$, $\eta_p^2 = 0.57$), as was the general adaptation effect ($t_{14} = 5.77$, $P = 0.001$, Cohen's D = 1.49; see Fig. 2D). Further pairwise posthoc comparisons revealed the same pattern of results as observed in PPA, OPA, and LO. Namely, for same judgments, there was a significant release from adaptation in the Same2 ($t_{14} = 3.59$, $P = 0.044$, Cohen's D = 0.93) and Same4 ($t_{14} = 6.60$, $P = 1.8 \times 10^{-4}$, Cohen's D = 1.70) conditions compared with the Same0 condition, and significantly greater activation in the Same4 condition compared with Same2 ($t_{14} = 4.07$, $P = 0.017$, Cohen's D = 1.05). For different judgments, the Different4 condition demonstrated significant adaptation compared with the Different0 ($t_{14} = 6.03$, $P = 4.6 \times 10^{-4}$, Cohen's D = 1.56) and Different2 ($t_{14} = 4.88$, $P = 0.004$, Cohen's D = 1.26) conditions, which did not differ ($t_{14} = 1.48$, $P > 0.99$, Cohen's D = 0.38; see Fig. 2D). Overall results in PPC1 were significantly different from those observed in PPA, LO, RSC, EVC, and FFA (all *F*s > 2.58, all *P*s < 0.04, all η_p^2s > 0.15), but not OPA ($F_{5,65} = 0.38$, $P = 0.86$, $\eta_p^2 = 0.03$), demonstrating that PPC1 is significantly different both from regions that do (i.e., PPA, LO) and do not (RSC, EVC, FFA) show an outlier effect. It is possible that the larger difference between adaptation conditions in PPC1 (i.e., Same0 vs. Same2; Different0 vs. Different2; Different2 vs. Different4) compared with PPA and LO may be driving the significant interaction between regions that both demonstrate outlier sensitivity. Furthermore, it is possible that dorsal regions may in general show greater sensitivity to outliers than ventral regions, likely due to dorsal regions' greater role in attention and task-related processing (see Xu, 2018a, 2018b).

The second region, PPC2, was localized using the adaptation data from all 15 participants and was defined as a region that showed greater activation for all 6 adaptation conditions compared with baseline fixation (i.e., an orthogonal contrast that does not bias activation in any one adaptation condition over another). A group-level analysis was used here because this region could not be reliably localized in each individual participant and the location of this ROI differed from that of PPC1. This region was then projected onto each participant's brain, and differences between the adaptation conditions were assessed separately for each participant. There was no evidence of hemispheric differences in activation ($F_{5,70} = 0.79$, $P = 0.56$, $\eta_p^2 = 0.05$), so data from the right and left hemispheres was collapsed. The main effect of Condition was significant ($F_{5,70} = 9.22$, $P = 8.9 \times 10^{-7}$, $\eta_p^2 = 0.40$), and the pairwise comparison denoting the general adaptation effect (i.e., Different0 > Same0) was also significant ($t_{14} = 3.66$, $P = 0.039$, Cohen's D = 0.94). Pairwise posthoc comparisons further investigating outlier sensitivity revealed results very similar to those observed in PPC1. Specifically, there was a significant release from adaptation in the Same4 ($t_{14} = 4.76$, $P = 0.005$, Cohen's D = 1.23) and Same2 ($t_{14} = 4.45$, $P = 0.008$, Cohen's D = 1.15) conditions compared with the Same0 condition, but these former two conditions did not differ ($t_{14} = 1.71$, $P > 0.99$, Cohen's D = 0.44; see Fig. 2D). For different judgments, the Different4 condition demonstrated significant adaptation compared with the Different0 ($t_{14} = 3.89$, $P = 0.024$, Cohen's D = 1.00) and Different2 ($t_{14} = 4.09$, $P = 0.016$, Cohen's D = 1.06) conditions, which did not differ ($t_{14} = 0.58$, $P > 0.99$, Cohen's D = 0.15). Not surprisingly, there were no significant differences observed when directly comparing the results in PPC1 and PPC2 ($F_{5,70} = 0.79$, $P = 0.56$, $\eta_p^2 = 0.05$).

In summary, two separate regions of PPC, localized using independent sets of imaging data, demonstrated the same sensitivity to processing ensemble outliers. These results are entirely consistent with the results from the ROI and whole-brain analyses reported above. See Table 2 for a summary of all of the main statistical results for the ROIs showing strong, weak, and no outlier effects, and Table 3 for a summary of the region-by-condition interaction results for all possible ROI combinations.

(6) Behavioral Results

The behavioral results for the adaptation runs, where participants were asked to ignore any outliers and judge whether two successively presented ensemble images (containing 0, 2, or 4 outliers) were mostly the same or mostly different, are presented in Table 4. For accuracy, the main effect of Condition was not significant ($F_{5,70} = 1.59$, $P = 0.18$, $\eta_p^2 = 0.10$), and no posthoc pairwise comparison reached significance (all *t*s < 2.08, all *P*s > 0.85, all Cohen's Ds < 0.54; see Fig. 4A). For response latency of the correct trials, the main effect of Condition was significant

Table 2

Summary of statistical results for regions demonstrating strong, weak, and no outlier effects.

Cortical Region	Hemisphere-by-Condition Interaction	Main Effect of Condition	General Adaptation Effect (Different0 > Same0)	Number of Significant Posthoc Comparisons for Outlier Effect (/6)	Significant Region-by-Condition Interactions
Strong Outlier Effect					
PPA	*NS*	$P = 2.0 \text{ x } 10^{-12}$	$P = 0.001$	4	RSC, FFA, PPC1,
OPA	*NS*	$P = 4.1 \text{ x } 10^{-13}$	$P = 0.003$	5	RSC, EVC, FFA
LO	*NS*	$P = 1.57 \text{ x } 10^{-10}$	$P = 0.004$	4	RSC, FFA, PPC1
PPC1	*NS*	$P = 10.00 \text{ x } 10^{-12}$	$P = 0.001$	5	PPA, RSC, EVC, LO, FFA
PPC2	*NS*	$P = 8.9 \text{ x } 10^{-7}$	$P = 0.039$	3	RSC, FFA
Weak Outlier Effect					
EVC	*NS*	$P = 3.3 \text{ x } 10^{-4}$	*NS*	1	RSC, OPA, PPC1
FFA	*NS*	$P = 4.50 \text{ x } 10^{-5}$	*NS*	2	PPA, RSC, OPA, LO, PPC1, PPC2
No Outlier Effect					
Combined RSC	$P = 0.03$	*NS*	*NS*	0	PPA, OPA, EVC, LO, FFA, PPC1, PPC2
Left RSC		*NS*	*NS*	0	PPA, OPA, EVC, LO, FFA, PPC1, PPC2
Right RSC		$P = 0.032$	*NS*	0	PPA, OPA, EVC, LO, FFA, PPC1, PPC2

PPA = parahippocampal place area; OPA = occipital place area; LO = lateral occipital area; PPC1 = posterior parietal cortex region 1; PPC2 = posterior parietal cortex region 2; EVC = early visual cortex; FFA = fusiform face area; RSC = retrosplenial complex; *NS* = not significant.

($F_{5,70} = 10.99$, $P = 7.9 \times 10^{-8}$, $\eta_p^2 = 0.44$), as was the pairwise comparison investigating the general adaptation effect ($t_{14} = 5.70$, $P = 0.001$, Cohen's D = 1.47). However, pairwise posthoc comparisons for same judgments revealed marginally significant faster responses in the Same0 condition compared with both the Same2 ($t_{14} = 3.38$, $P = 0.067$, Cohen's D = 0.87) and Same4 ($t_{14} = 3.53$, $P = 0.05$, Cohen's D = 0.91) conditions, which did not differ ($t_{14} = 2.23$, $P = 0.64$, Cohen's D = 0.58). For different judgments, responses in the Different4 condition were significantly faster than those in the Different0 condition ($t_{14} = 4.17$, $P = 0.014$, Cohen's D = 1.08), but all other comparisons were not significant (Different4 vs. Different2: $t_{14} = 2.67$, $P = 0.28$, Cohen's D = 0.69; Different2 vs. Different0: $t_{14} = 1.91$, $P > 0.99$, Cohen's D = 0.49; see Fig. 4A).

While we did find some significant effects in our behavioral measures (i.e., response latency), we do not believe that our fMRI adaptation response patterns are simply a reflection of the behavioral responses, for a few reasons. First, the pattern of significant pairwise comparisons in the accuracy and response latency analyses do not fully match the pattern of significant pairwise comparisons in the fMRI adaptation analysis (i.e., Same2 and Same4 significantly differ in PPA, OPA, and LO, but these conditions do not differ in accuracy or response latency; Different2 and Different4 significantly differ in PPA, OPA, and LO, but these conditions do not differ in accuracy or response latency). In fact, we found a significant interaction in a two-way ANOVA with Measurement (behavioral response latency vs PPA fMRI response) and Condition (6 adaptation conditions) as factors ($F_{5,\ 70} = 3.59$, $P = 0.006$, $\eta_p^2 = 0.20$). Second, we split the behavioral and neuroimaging data into two groups based on whether they show a weak (i.e., decreasing or flat response latencies in same trials as outliers are introduced and/or increasing or flat response latencies in different trials as outliers are introduced) or strong (i.e., increasing response latencies in same trials as outliers are introduced, and decreasing response latencies in different trials as outliers are introduced; in other words, when response latencies matched the pattern of neural response observed for the outlier effect) response latency effect to examine whether the neural data can be explained by differences in response latency. Specifically, we analyzed each data set using a 2 (Group: weak response latency effect vs. strong response latency effect) by 6 (Condition: 6 adaptation conditions) mixed model ANOVA. As expected, we found a significant difference between the two groups in response latency (i.e., a significant Group-by-Condition interaction: $F_{5,65} = 4.04$, $P = 0.003$, $\eta_p^2 = 0.24$), but found no differences in the accuracy data ($F_{5,65} = 0.54$, $P = 0.75$, $\eta_p^2 = 0.04$; see Fig. 4B), and importantly, no group differences were observed in any brain region (i.e., the Group-by-Condition interaction was not significant in PPA, LO, OPA, RSC, EVC, FFA, PP1, and PP2: all Fs < 1.55, all Ps > 0.19, all η_p^2s < 0.12). This is particularly telling in the data from PPA and LO: While the two groups showed very different RT patterns (see Fig. 4B, right), virtually the same activation patterns were found in PPA and LO in both groups (see Fig. 4C). This is strong evidence that our neural adaptation results cannot be explained by differences in response latency and cognitive strategy (i.e., a speed-accuracy trade-off) across the conditions. Finally, and importantly, findings by Xu et al. (2007) showed that fMRI adaptation responses in PPA are dissociable from behavioral responses, which is consistent with the present series of results as well as with our previous studies, which all utilized a fast event-related adaptation paradigm (Cant and Xu, 2012, 2015, 2017; Lowe et al., 2017).

Finally, to investigate if the group-level whole-brain results could be explained by differences in behavioral performance across our participants, we conducted the whole-brain conjunction analysis (see 'The processing of outliers across the entire brain' section) separately on the participants who showed a strong (N = 8) or weak (N = 7) behavioral response latency effect. Specifically, in each sub-group separately, we looked for regions that showed the conjunction of increased activation in the Same4 condition compared with the Same0 condition, and increased activation in the Different0 condition compared with the Different4 condition. Overall, we see very similar activations across the two sub-groups (i.e., bilateral activation in parahippocampal cortex near PPA, fusiform gyrus, OPA, IPS, and SPL; all $P < 0.05$, uncorrected; see Fig. 3B and Table 1). The fact that very similar results are observed across the two sub-groups makes it unlikely that the whole-brain random-effects results for the entire group can be explained by differences in response latency and cognitive strategy, which is consistent with the results we found with the adaptation data in single participants.

4. Discussion

The results of this study demonstrate two main findings with regard to object-ensemble representation in the human brain. First, we have evidence that ensemble representation in anterior-medial ventral visual cortex is sensitive to the presence of outliers, likely because they change the nature of an otherwise homogeneous ensemble. Specifically, with just 4 outliers in same judgment trials, we observed a significant release from adaptation in PPA (the effect was marginally significant with 2 outliers), comparable to when two completely different ensembles were presented.

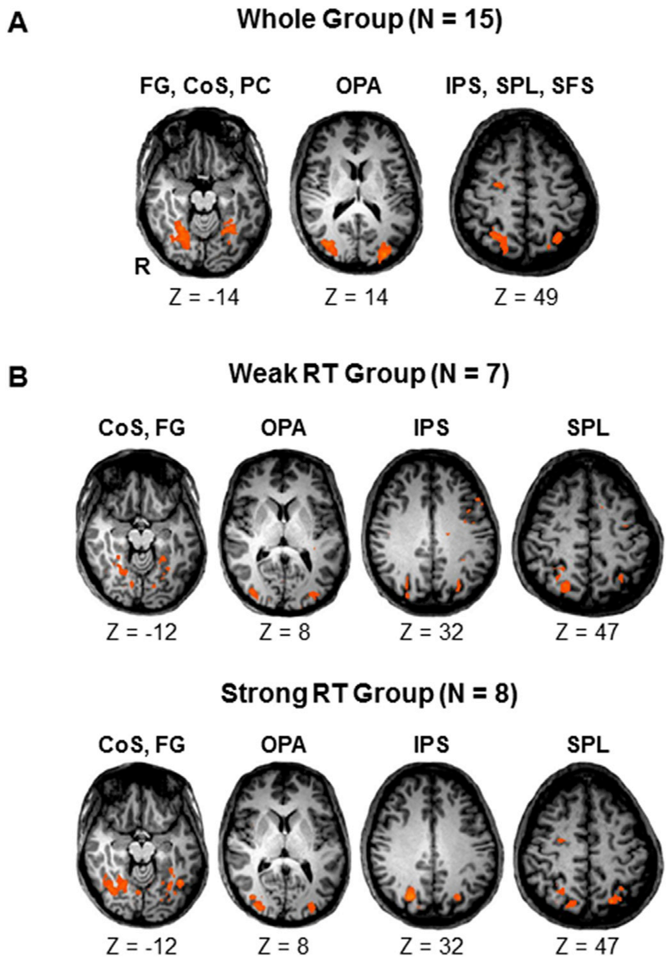

Fig. 3. Results of the whole-brain random-effects analyses. **A.** Results ($N = 15$) of the whole-brain random-effects analysis on the entire group of participants. A conjunction analysis searching for regions that showed increased activation in the Same4 condition compared with the Same0 condition, and increased activation in the Different0 condition compared with the Different4 condition (i.e., the two strongest adaptation effects observed in the ROI analysis) revealed activation in occipital, temporal, parietal, and frontal cortices (all $P < 0.01$, uncorrected). **B.** Results of the whole-brain random-effects analyses for the weak ($N = 7$) and strong ($N = 8$) response latency groups. A conjunction analysis searching for regions that showed increased activation in the Same4 condition compared with the Same0 condition, and increased activation in the Different0 condition compared with the Different4 condition (i.e., the two strongest adaptation effects observed in the ROI analysis), returned very similar results across the two sub-groups, with activations concentrated mostly in occipital, temporal, and parietal cortices (all $P < 0.05$, uncorrected). This makes it unlikely that the whole-brain random-effects results for the entire group can be explained by differences in response latency and cognitive strategy. R = right hemisphere; OPA = occipital place area; FG = fusiform gyrus; CoS = collateral sulcus; PC = parahippocampal cortex; IPS = intraparietal sulcus; SPL = superior parietal lobule; SFS = superior frontal sulcus; RT = reaction time.

Moreover, with just 4 outliers in different judgment trials, we observed significant adaptation in PPA, comparable to when the same homogeneous ensemble (i.e., no outliers) was repeated. Thus, outliers significantly impact the representation of otherwise homogeneous ensembles in human anterior-medial ventral visual cortex. Second, this sensitivity is not confined to a single region of the ventral stream, but is observed in regions of occipito-temporal cortex that are involved in both ensemble and shape processing (i.e., PPA, OPA and LO; see below for a more detailed discussion of OPA). Furthermore, the sensitivity to processing ensemble outliers is not confined only to occipito-temporal cortex, as the results of the whole-brain random effects analysis revealed sensitivity to processing ensemble information in task-related regions in posterior parietal, and to a lesser extent, frontal cortices, which is consistent with a recent fMRI study investigating ensemble facial emotion processing (Im et al., 2017; but see below). This neural outlier sensitivity is not a mere reflection of behavioral responses, since the same outlier effect was observed whether or not there was a strong or weak outlier modulation of behavioral responses. Overall, these results demonstrate that sensitivity to processing ensemble outliers is present in brain regions involved in the sensory and the task-related aspects of ensemble stimulus processing. This may speak to the adaptive and beneficial nature of outlier processing, since perceptual sensitivity to deviants can confer a behavioral advantage in multiple scenarios (e.g., seeing a bad apple in a bushel, detecting a threatening face in a crowd, etc.). To our knowledge, this is the first time an outlier effect has been systematically documented in the human brain. Such an outlier effect could well provide the neural basis of outlier perception.

Table 3
Summary of region-by-condition interaction results for all ROIs.

	PPA	RSC	OPA	EVC	LO	FFA	PPC1	PPC2
PPA		$P = 2.0 \times 10^{-6}$	*NS*	*NS*	*NS*	$P = 0.009$	$P = 0.02$	*NS*
RSC			$P = 9.7 \times 10^{-8}$	$P = 0.02$	$P = 2.0 \times 10^{-6}$	$P = 0.001$	$P = 6.2 \times 10^{-8}$	$P = 0.001$
OPA				$P = 0.01$	*NS*	$P = 5.0 \times 10^{-4}$	*NS*	*NS*
EVC					*NS*	*NS*	$P = 0.002$	*NS*
LO						$P = 0.009$	$P = 0.03$	*NS*
FFA							$P = 6.0 \times 10^{-6}$	$P = 0.02$
PPC1								*NS*
PPC2								

PPA = parahippocampal place area; RSC = retrosplenial complex; OPA = occipital place area; EVC = early visual cortex; LO = lateral occipital area; FFA = fusiform face area; PPC1 = posterior parietal cortex region 1; PPC2 = posterior parietal cortex region 2; *NS* = not significant.

In our prior studies, we documented ensemble representation in PPA and its sensitivity to the shape and texture of ensemble elements as well as the ratio and identity of the different objects comprising a heterogeneous ensemble (Cant and Xu, 2012, 2015, 2017). Here we show that PPA also exhibits sensitivity to the presence of outliers in an ensemble, providing further support for PPA's involvement in object ensemble processing. Although LO has been largely associated with the processing of the shape of single objects (Grill-Spector et al., 1999; Kourtzi and Kanwisher, 2001; Malach et al., 1995; Williams et al., 2007), we previously showed that LO is also sensitive to processing shape changes of ensemble elements (Cant and Xu, 2012, 2015, 2017). This could account for the outlier effect we found here in LO, as the presence of outliers signals a salient and significant shape change. In our previous studies, OPA exhibited some sensitivity to shape changes in ensemble elements, although this response has in general been weak and less consistent across experiments (Cant and Xu, 2012, 2015, 2017). The outlier effect found in OPA here could reflect some shape processing of the ensemble elements, as opposed to that in PPA which is likely based on a more global statistical extraction of ensemble elements and outliers. Furthermore, these outlier effects may be used for different aspects of scene processing related to the functional dissociation between these two regions (Walther et al., 2009; Persichetti and Dilks, 2018, 2019). Specifically, outlier detection may aid scene categorization in PPA but scene navigation in OPA. More research is needed to fully understand the interaction between outlier detection and scene processing in PPA and OPA.

Table 4

Percent correct accuracies and response latencies (in ms) of correct trials for the adaptation runs. All values represent means with standard errors.

	Same – 0 Outliers	Same – 2 Outliers	Same – 4 Outliers	Different – 0 Outliers	Different – 2 Outliers	Different – 4 Outliers
Accuracy	94.05 ± 2.38	94.76 ± 1.70	96.19 ± 1.01	96.91 ± 1.43	96.67 ± 1.07	94.76 ± 1.43
Response Latency	785 ± 30	823 ± 32	843 ± 32	875 ± 29	852 ± 31	821 ± 30

Why do we consistently see sensitivity to processing ensemble stimuli in scene- and texture-selective cortex? Ensemble representation requires the encoding of the summary statistics of an ensemble without representing in detail each element comprising the ensemble. Likewise, in scene perception, the gist of a scene may be extracted without encoding the detailed features of each object in the scene, and in texture perception, the global texture percept may be extracted without encoding every texture element in detail. The ensemble outlier effect we report in the present study may be based on a comparison of global and local properties in successive ensemble displays, which is consistent with previous findings demonstrating an interaction across these different levels of ensemble representation (e.g., Brady and Alvarez, 2011). It is because of these processing similarities that we believe ensemble, scene, and texture perception are representationally linked in PPA, even though the ensembles we used in all of our prior studies (Cant and Xu, 2012, 2015, 2017) and in the current experiment contained no 3D spatial or scene information. Support for the processing of texture in scene-selective cortex has come from recent human (Park and Park, 2017; Henriksson et al., 2019) and monkey (Kornblith et al., 2013) fMRI studies. Our results contribute to this growing body of literature by demonstrating an additional link with ensemble processing, underscoring the computational similarities in processing all three seemingly distinct types of stimuli.

It is not obvious a priori that outliers would always be processed. Previous behavioral studies of ensemble processing have shown that outliers are discounted in the statistical processing of facial expression (Haberman and Whitney, 2010). There are also ample cases in which distractor locations and features can be effectively inhibited and minimally processed using location and feature-based attentional selection mechanisms (Posner, 1980; Maunsell and Treue, 2006). In our study, if the second display is taken as a whole, then from an image similarity point of view, the second image would be more similar to the first image when only a few items changed (e.g., the Same2 and Same4 conditions). The fact that our ensemble displays were not processed in this manner and that outliers were amplified rather than effectively suppressed reveals an interesting brain mechanism that, to our knowledge, has not been previously documented. Our neural results demonstrate that discounting outliers in statistical processing of facial expression as reported by Haberman and Whitney (2010) must be occurring at a later stage of processing, as the visual system appears to be quite sensitive to the presence of outliers. Indeed, in the present study we chose a task that required the suppression of outlier processing, yet we found that outliers

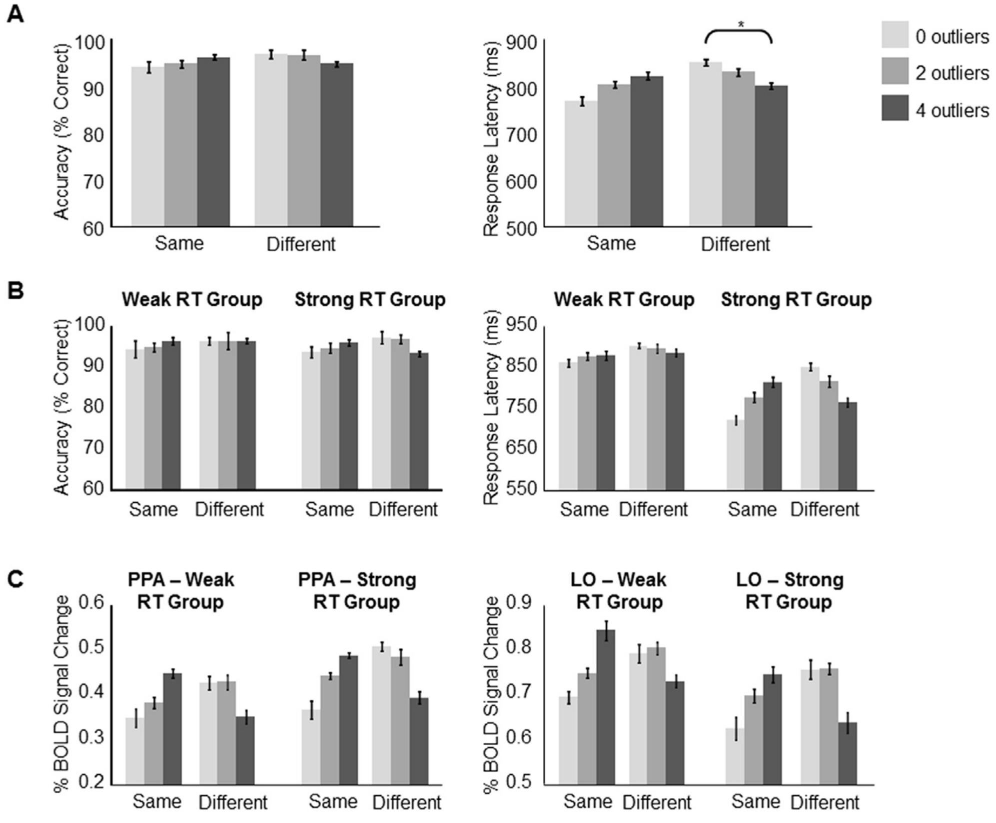

Fig. 4. Behavioral results for all six outlier conditions and the effect of the strength of response latency on fMRI adapatation. **A.** Overall (N = 15) accuracy and response latency results. No differences in accuracy were observed across the six conditions, and only one significant difference was observed in the response latency data, demonstrating that the pattern of significant pairwise comparisons does not fully match the pattern of significant pairwise comparisons in the fMRI adaptation analysis in the ROIs that showed a strong outlier effect (i.e., PPA, LO, OPA, PPC1, and PPC2). **B.** Accuracy and response latency data grouped by strength of response latency effect. Splitting the behavioral data into two groups based on whether participants showed a weak or strong response latency effect reveals no difference between the groups for accuracy, but, as expected, the groups differed significantly in terms of response latency. **C.** fMRI adaptation data grouped by strength of response latency effect. While the two groups showed very different response latency patterns, there were no group differences in the activation patterns observed in PPA and LO (the same result was also observed in RSC, OPA, EVC, FFA, PPC1, and PPC2; data not shown here). This strongly suggests that the neural adaptation results cannot be explained by differences in response latency and cognitive strategy across the conditions. Error bars represent within-subject standard errors (i.e. with the between-subject variation removed; see Loftus and Mason, 1994). PPA = parahippocampal place area; LO = lateral occipital area; ms = milliseconds; RT = reaction time; BOLD = blood oxygen level dependent; * $P < 0.05$.

still dominated neural representation in multiple regions. This seems to suggest that when outliers are ignored, it happens quite late at the decision stage of processing, rather than at the perceptual stage.

The PFC and PPC form the task-positive (Fox et al., 2005) or multiple demand (MD) network (Duncan, 2010), which are a set of brain regions long known to be involved in the performance of a variety of tasks, supporting functions such as attention, task control, working memory and decision-making. These brain regions have been additionally shown to be able to directly represent task-related visual information (e.g., Christophel et al., 2017; Xu, 2018a, 2018b). In our study, outliers are likely represented in these task-related regions so that they may be actively discounted to produce the correct task response. Although our study does not provide direct neural evidence for this outlier discounting, prior studies have highlighted the role of the anterior cingulate cortex in conflict monitoring and resolution (e.g., Botvinick et al., 2004). More detailed studies involving PFC's role in decision making are needed to fully understand how outliers may be discounted.

We believe that the choice of our experimental task was an important consideration when investigating ensemble outlier processing. For example, since distinctive outliers can capture attention, using an orthogonal task with no explicit instructions on whether to attend or ignore outliers may have led participants to pay attention to the outliers rather than actively ignore them, especially when doing so may not impact behavior. If this were the case, then any outlier effect observed could be attributed to participants attending to the outliers only. For this reason, we specifically chose a task that required participants to actively ignore outliers in the second display and judge whether the two ensemble displays were mostly the same or different. Thus it was to the participants' advantage to ignore the outliers rather than fixating on them and ignoring the rest of the display. Since the outliers were the minority, we reasoned that participants could quickly extract the identity of the majority of the ensemble items and easily ignore the outliers. The high performance accuracy we obtained showed that participants were successful in doing so. Our same- and different-judgement task thus works against finding any adaptation effect based on the outliers. The fact that we still found a significant outlier effect in multiple regions shows that despite participants paying attention to the whole display and actively ignoring the outliers, outlier processing is still robust and appears to be automatic. Such resilience to top-down suppression based on task demands further speaks to the strength of the outlier processing effect. Consequently, by actively suppressing top-down attention in outlier processing, we believe the task we employed made our findings much more interesting and informative compared with using an orthogonal task.

Without top-down attention at play, our neural outlier effect is likely driven by a bottom-up effect. However, our outlier effect is not simply an attentional saliency effect with the presence of outliers grabbing attention and resulting in a higher neural response. This is because with just 4 outliers in different judgment trials, we observed significant adaptation (i.e., a lower response) in a number of brain regions, comparable to when the same homogeneous ensemble (i.e., no outliers) was repeated. In other words, the saliency of the outliers rendered two otherwise distinctive displays as indistinguishable using our adaptation measure. This indicates that it was the match/mismatch between the identities of the outliers and the items in a preceding homogeneous display that was driving the effect and not merely the salient presence of the outliers. Put differently, the outlier effect reflects the representational distance between the first and second ensemble displays. That is, the presence of outliers leads to a release from adaptation as the representational distance between the first and second displays increases (i.e., the number of identical objects between the displays decreases), whereas outliers lead to adaptation when the representational distance between the ensembles decreases (i.e., the number of identical objects increases). Thus, the computation of representational distance may be one way that ensemble processing mechanisms flag the presence of outliers in the visual array.

Although the overall response pattern of the outlier effect appeared to be present across the ROIs we investigated, its strength varied considerably. Specifically, PPA, LO, OPA, PPC1, and PPC2 showed the strongest outlier effects (all showing a significant outlier effect in 4 or more of the 6 possible pairwise comparisons), whereas FFA, EVC, and RSC all showed much weaker or no (i.e., statistically non-significant) outlier effects (showing a significant outlier effect in only 2 or less of the 6 possible pairwise comparisons), with some of the stronger regions showing a significant interaction with EVC. As discussed earlier, PPA, LO and OPA were directly involved in processing the ensemble and shape information present in the stimuli, while PPC regions were associated with task-related processing. Meanwhile, although RSC showed an overall lower activation to the ensemble stimuli, the overall responses of FFA were equally high as those of PPA and OPA, and those of EVC were the highest among all the regions. Yet despite the ensemble stimuli evoking significant responses in FFA and EVC, these brain regions showed weak outlier effects. Thus the robust outlier effect we observed in the other regions is not a general effect present in all visually responsive brain regions; but rather, it is limited to brain regions more closely involved in the sensory and task-related aspects of ensemble processing. Given the close interconnection among the different visual regions, weaker outlier effects observed in RSC, FFA and EVC are likely due to feedback signals propagating from regions more involved in ensemble and shape processing.

While bottom-up attention is certainly playing a role in outlier processing, we want to emphasize that the outlier effect we observed here is not a general effect explained solely by general attentional mechanisms. As described above, the ROIs showing strong outlier sensitivity are not an arbitrary set of regions. But rather, they are regions closely involved in ensemble and shape processing in occipito-temporal cortex, and task-related processing in fronto-parietal cortex. Moreover, as discussed earlier, our outlier effect is not a saliency effect with a brain region simply showing a higher response to the presence of the salient outliers. Instead, depending on whether the first display contains elements that do or do not match the outlier elements in the second display, the overall brain response could either be lower (i.e., adaptation) or higher (i.e., release from adaptation), respectively. Thus for any brain region to show the outlier effect, it needs to not only encode the ensemble stimuli but also show sensitivity to the difference between the ensemble and outlier elements. It is unclear how brain regions not sensitive to ensemble, shape, or task-related processing would show an outlier effect and how a general attention mechanism can account for these findings.

Furthermore, we do not believe that our results are idiosyncratic to our analytical technique and experimental design (i.e., fMR-adaptation using a fast event-related protocol), and instead represent a more general cognitive and neural phenomenon. Although differences between fMRI adaptation and multivoxel pattern analysis (MVPA) have been noted and have been attributed to reflecting representation at different scales (e.g., within-versus across-voxels within a region; see Park and Park, 2017), there still exist a large number of results that are consistent between these two methods, such as showing sensitivity to object identity changes (e.g., Grill-Spector et al., 1999; Kourtzi and Kanwisher, 2001; Haxby et al., 2001; Williams et al., 2007). As such, we predict similar results in a study optimally designed to use MVPA. Specifically, in outlier-sensitive regions (i.e., PPA, OPA, LO, PPC), we predict that a linear support vector machine (SVM) classifier would successfully distinguish between the activation patterns associated with displays containing 0, 2 and 4 outliers. Further studies are needed to confirm these predictions.

In a recent study, by contrasting a task involving ensemble coding of crowd emotion with a task involving the processing of emotion from individual faces, Im et al. (2017) found that regions in PPC and PFC exhibited higher fMRI responses in the ensemble face-coding task than the individual face-coding task. However, ensemble face coding required the processing of multiple stimuli occupying a larger visual field than the coding of an individual face (which was matched in size to the faces shown in the face ensemble). Thus, higher PPC and PFC responses could reflect this initial encoding demand and not necessarily neural processing specific to ensemble representation. Consistent with this account, early visual areas also showed a higher response to ensemble than individual face coding (see Fig. 4A of Im et al., 2017). By matching the visual field coverage of different types of stimuli and using fMRI adaptation in the present study, we were able to show unambiguously the direct involvement of posterior parietal and frontal cortices in ensemble outlier representation. These results are consistent with the role of these brain regions in task-related processing and, together with the results found in ventral visual regions, delineate the key regions involved in outlier processing in the human brain.

What do our current results investigating outliers contribute to our understanding of ensemble representation in these brain regions? Given that ensembles usually contain large numbers of objects, 2 (and possibly 4) outliers may be represented as individuals rather than as an ensemble. However, they may be grouped together, due to shared visual or semantic features. Our results suggest that 4 outliers perceptually grouped together may indeed be represented as an ensemble, since the most consistent finding in all outlier-sensitive regions was comparable releases from adaptation in Same4 and Different0 trials, and comparable adaptation in Same0 and Different4 trials. In anterior-medial ventral visual cortex, it appears that the same neurons that normally represent the larger ensembles are recruited to encode the outliers in that the overall neural response in this region is dominated by the presence of outliers in the second display, in relation to the previously seen ensemble containing no outliers. This is interesting, as it demonstrates that ensemble-sensitive regions such as PPA are able to code ensemble features at both global (i.e., entire set-level visual similarity and dissimilarity) and local (i.e., outlier detection) levels of representation. As discussed earlier, in other brain regions that do not routinely show global-based ensemble sensitivity (e.g., OPA, LO), the adaptation results are likely driven by individual object or feature (e.g., shape) perception across both ensemble displays. In task-related regions such as frontal and posterior parietal cortices, it is likely that outliers are represented in order to be actively discounted to produce the correct task response. Thus different brain regions work in concert to ensure that outliers are detected and then processed appropriately according to the goal of the task at hand (e.g., either discounted or enhanced).

5. Conclusions

To conclude, we present evidence that both ensemble- and shape-processing sensory regions, as well as task-related processing regions show sensitivity to the presence of outliers in object ensembles. These neural mechanisms likely work together to flag the presence of outliers during visual perception and then weigh the outliers appropriately in subsequent decisions relating to behavioral task demands. After all, the mechanisms responsible for perceiving the entire forest and the individual trees from the same scene should both be sensitive to the presence of one or two trees that are on fire, and should then be able to pass this information on to fronto-parietal task-related regions so that an appropriate action may be taken.

Declaration of competing interest

None.

CRediT authorship contribution statement

Jonathan S. Cant: Conceptualization, Methodology, Validation, Formal analysis, Investigation, Data curation, Writing - original draft, Writing - review & editing, Visualization. **Yaoda Xu:** Conceptualization, Methodology, Software, Validation, Resources, Writing - review & editing, Visualization, Supervision, Project administration, Funding acquisition.

Acknowledgments

This research was supported by grants from the US National Institutes of Health (1R01EY022355) to Y.X., and a Canadian Natural Sciences and Engineering Research Council Postdoctoral Fellowship and Discovery Grant (435647) to J.S.C. We thank Su Keun Jeong and Jiedong Zhang for help with data collection. The authors have no competing interests to declare.

Appendix A. Supplementary data

Supplementary data to this article can be found online at https://doi.org/10.1016/j.neuroimage.2020.116629.

References

Ariely, D., 2001. Seeing sets: representation by statistical properties. Psychol. Sci. 12, 157–162.

Balas, B., Nakano, L., Rosenholtz, R., 2009. A summary-statistic representation in peripheral vision explains visual crowding. J. Vis. 9 (12), 1–18, 13.

Botvinick, M.M., Cohen, J.D., Carter, C.S., 2004. Conflict monitoring and anterior cingulate cortex: an update. Trends Cognit. Sci. 8 (12), 539–546.

Brady, T.F., Alvarez, G.A., 2011. Hierarchical encoding in visual working memory: ensemble statistics bias memory for individual items. Psychol. Sci. 22 (3), 384–392.

Brainard, D.H., 1997. The psychophysics toolbox. Spatial Vis. 10, 433–436.

Cant, J.S., Goodale, M.A., 2007. Attention to form or surface properties modulates different regions of human occipitotemporal cortex. Cerebr. Cortex 17, 713–731.

Cant, J.S., Arnott, S.R., Goodale, M.A., 2009. fMR-adaptation reveals separate processing regions for the perception of form and texture in the human ventral stream. Exp. Brain Res. 192, 391–405.

Cant, J.S., Goodale, M.A., 2011. Scratching beneath the surface: new insights into the functional properties of the lateral occipital area and parahippocampal place area. J. Neurosci. 31, 8248–8258.

Cant, J.S., Xu, Y., 2012. Object ensemble processing in human anterior-medial ventral visual cortex. J. Neurosci. 32, 7685–7700.

Cant, J.S., Xu, Y., 2015. The Impact of density and ratio on object-ensemble representation in human anterior-medial ventral visual vortex. Cerebr. Cortex 25, 4226–4239.

Cant, J.S., Xu, Y., 2017. The contribution of object shape and surface properties to object ensemble representation in anterior-medial ventral visual cortex. J. Cognit. Neurosci. 29 (2), 398–412.

Christophel, T.B., Klink, P.C., Spitzer, B., Roelfsema, P.R., Haynes, J.D., 2017. The distributed nature of working memory. Trends Cognit. Sci. 21 (2), 111–124.

Dakin, S.C., Watt, R.J., 1997. The computation of orientation statistics from visual texture. Vis. Res. 37 (22), 3181–3192.

de Fockert, J.W., Wolfenstein, C., 2009. Rapid extraction of mean identity from sets of faces. Q. J. Exp. Psychol. 62 (9), 1716–1722.

Dilks, D.D., Julian, J.B., Kubilius, J., Spelke, E.S., Kanwisher, N., 2011. Mirror-image sensitivity and invariance in object and scene processing pathways. J. Neurosci. 31, 11305–11312.

Dilks, D.D., Julian, J.B., Paunov, A.M., Kanwisher, N., 2013. The occipital place area is causally and selectively involved in scene perception. J. Neurosci. 33 (4), 1331–1336.

Duncan, J., 2010. The multiple-demand (MD) system of the primate brain: mental programs for intelligent behaviour. Trends Cognit. Sci. 14 (4), 172–179.

Epstein, R.A., Higgins, J.S., 2007. Differential parahippocampal and restrosplenial involvement in three types of visual scene recognition. Cerebr. Cortex 17, 1680–1693.

Epstein, R., Kanwisher, N., 1998. A cortical representation of the local visual environment. Nature 392, 598–601.

Fox, M.D., Snyder, A.Z., Vincent, J.L., Corbetta, M., Van Essen, D.C., Raichle, M.E., 2005. The human brain is intrinsically organized into dynamic, anticorrelated functional networks. Proc. Natl. Acad. Sci. Unit. States Am. 102 (27), 9673–9678.

Friston, K.J., Homes, A.P., Worsley, K.J., Poline, J.-P., Frith, C.D., Frackwowiak, R.S.J., 1995. Statistical parametric maps in functional imaging: a general linear model approach. Hum. Brain Mapp. 2, 189–210.

Grill-Spector, K., Kushnir, T., Edelman, S., Avidan, G., Itzchak, Y., Malach, R., 1999. Differential processing of objects under various viewing conditions in the human lateral occipital complex. Neuron 24 (1), 187-20.

Grill-Spector, K., Kushnir, T., Hendler, T., Malach, R., 2000. The dynamics of object-selective activation correlate with recognition performance in humans. Nat. Neurosci. 3, 837–843.

Haberman, J., Whitney, D., 2007. Rapid extraction of mean emotion and gender from sets of faces. Curr. Biol. 17 (7), 751–753.

Haberman, J., Whitney, D., 2010. The visual system discounts emotional deviants when extracting average expression. Atten. Percept. Psychophys. 72 (7), 1825–1838.

Haxby, J.V., Gobbini, M.I., Furey, M.L., Ishai, A., Schouten, J.L., Pietrini, P., 2001. Distributed and overlapping representations of faces and objects in ventral temporal cortex. Science 293 (5539), 2425–2430.

Henriksson, L., Mur, M., Kriegeskorte, N., 2019. Rapid invariant encoding of scene layout in human OPA. Neuron 103, 161–171.

Hochstein, S., Pavlovskaya, M., Bonneh, Y.S., Soroker, N., 2018. Comparing set summary statistics and outlier pop out in vision. J. Vis. 18 (13), 12-12.

Im, H.Y., Albohn, D.N., Steiner, T.G., Cushing, C.A., Adams, R.B., Kveraga, K., 2017. Differential hemispheric and visual stream contributions to ensemble coding of crowd emotion. Nat. Hum. Behav. 1 (11), 828–842.

Kanwisher, N., McDermott, J., Chun, M.M., 1997. The fusiform face area: a module in human extrastriate cortex specialized for face perception. J. Neurosci. 17, 4302–4311.

Khayat, N., Hochstein, S., 2018. Perceiving set mean and range: automaticity and precision. J. Vis. 18 (9), 1–14, 23.

Kornblith, S., Cheng, X., Ohayon, S., Tsao, D.Y., 2013. A network for scene processing in the macaque temporal lobe. Neuron 79 (4), 766–781.

Kourtzi, Z., Kanwisher, N., 2001. Representation of perceived object shape by the human lateral occipital complex. Science 293, 1506–1509.

Loftus, G.R., Mason, M.E.J., 1994. Using confidence intervals in within-subject designs. Psychon. Bull. Rev. 1 (4), 476–490.

Lowe, M.X., Rajsic, J., Gallivan, J.P., Ferber, S., Cant, J.S., 2017. Neural representation of geometry and surface properties in object and scene perception. Neuroimage 157, 586–597.

MacEvoy, S.P., Epstein, R.A., 2011. Constructing scenes from objects in human occipitotemporal cortex. Nat. Neurosci. 14 (10), 1323–1329.

Malach, R., Reppas, J.B., Benson, R.R., Kwong, K.K., Jiang, H., Kennedy, W.A., Ledden, P.J., Brady, T.J., Rosen, B.R., Tootell, R.B., 1995. Object-related activity revealed by functional magnetic resonance imaging in human occipital cortex. Proc. Natl. Acad. Sci. U. S. A. 92, 8135–8139.

Maunsell, J.H., Treue, S., 2006. Feature-based attention in visual cortex. Trends Neurosci. 29 (6), 317–322.

Ogawa, S., Tank, D.W., Menon, R., Ellermann, J.M., Kim, S.G., Merkle, H., Ugurbil, K., 1992. Intrinsic signal changes accompanying sensory stimulation: functional brain mapping with magnetic resonance imaging. Proc. Natl. Acad. Sci. U. S. A. 89, 5951–5955.

Oliva, A., Torralba, A., 2001. Modeling the shape of the scene: a holistic representation of the spatial envelope. Int. J. Comput. Vis. 42, 145–175.

Park, J., Park, S., 2017. Conjoint representation of texture ensemble and location in the parahippocampal place area. J. Neurophysiol. 117 (4), 1595–1607.

Pelli, D.G., 1997. The VideoToolbox software for visual psychophysics: transforming numbers into movies. Spatial Vis. 10, 437–442.

Persichetti, A.S., Dilks, D.D., 2018. Dissociable neural systems for recognizing places and navigating through them. J. Neurosci. 38, 10295–10304.

Persichetti, A.S., Dilks, D.D., 2019. Distinct representations of spatial and categorical relationships across human scene-selective cortex. Proc. Natl. Acad. Sci. Unit. States Am. 116 (42), 21312–21317.

Peuskens, H., Claeys, K.G., Todd, J.T., Norman, J.F., Van Hecke, P., Orban, G.A., 2004. Attention to 3-D shape, 3-D motion, and texture in 3-D structure from motion displays. J. Cognit. Neurosci. 16, 665–682.

Posner, M.I., 1980. Orienting of attention. QJ Exp. Psychol. 32 (1), 3–25.

Rosenholtz, R., 2011. What your visual system see where you are not looking. In: Rogowitz, B.E., Pappas, T.N. (Eds.), Human Vision and Electronic Imaging XVI, vol. 7865, pp. 1–14.

Rosenholtz, R., Huang, J., Raj, A., Balas, B.J., Ilie, L., 2012. A summary statistic representation in peripheral vision explains visual search. J. Vis. 12 (4), 1–17, 14.

Rossion, B., Pourtois, G., 2004. Revisiting Snodgrass and Vanderwart's object pictorial set: the role of surface detail in basic-level object recognition. Perception 33, 217–236.

Saxe, R., Brett, M., Kanwisher, N., 2006. Divide and conquer: a defense of functional localizers. Neuroimage 30, 1088–1096 discussion 1097-1089.

Talairach, J., Tournoux, P., 1988. Co-planar Stereotaxic Atlas of the Human Brain. Thieme Medical Publishers, New York, NY.

Todd, J.J., Han, S.K., Harrison, S., Marois, R., 2011. The neural correlates of visual working memory encoding: a time-resolved fMRI study. Neuropsychologia 49, 1527–1536.

Todd, J.J., Marois, R., 2004. Capacity limit of visual short-term memory in human posterior parietal cortex. Nature 428, 751–754.

Treisman, A., Gelade, G., 1980. A feature-integration theory of attention. Cognit. Psychol. 12, 97–136.

Vaziri Pashkam, M., Xu, Y., 2017. Goal-directed visual processing differentially impacts human ventral and dorsal visual representations. J. Neurosci. 37, 8767–8782.

Walther, D.B., Caddigan, E., Fei-Fei, L., Beck, D.M., 2009. Natural scene categories revealed in distributed patterns of activity in the human brain. J. Neurosci. 29 (34), 10573–10581.

Whitney, D., Leib, A.Y., 2018. Ensemble perception. Annu. Rev. Psychol. 69, 12.1–12.25.

Williams, M.A., Dang, S., Kanwisher, N.G., 2007. Only some spatial patterns of fMRI response are read out in task performance. Nat. Neurosci. 10 (6), 685–686.

Xu, Y., 2010. The neural fate of task-irrelevant features in object-based processing. J. Neurosci. 30, 14020–14028.

Xu, Y., 2017. Reevaluating the sensory account of visual working memory storage. Trends Cognit. Sci. 21 (10), 794–815.

Xu, Y., 2018a. A tale of two visual systems: invariant and adaptive visual information representations in the primate brain. Annu. Rev. Vis. Sci. 4, 311–336.

Xu, Y., 2018b. The posterior parietal cortex in adaptive visual processing. Trends Neurosci. 41, 806–822.

Xu, Y., Chun, M.M., 2006. Dissociable neural mechanisms supporting visual short-term memory for objects. Nature 440, 91–95.

Xu, Y., Turk-Browne, N.B., Chun, M.M., 2007. Dissociating task performance from fMRI repetition attenuation in ventral visual cortex. J. Neurosci. 27, 5981–5985.

Yamanashi Leib, A., Kosovicheva, A., Whitney, D., 2016. Fast ensemble representations for abstract visual impressions. Nat. Commun. 7, 13186.